

Analysis and Control of a Transmission Model for Respiratory Syncytial Virus.

Lakshmi. N. Sridhar

Chemical Engineering Department, University of Puerto Rico, Mayaguez, PR 00681, Puerto Rico.

***Correspondence Author:** Dr. Lakshmi. N. Sridhar, Chemical Engineering Department, University of Puerto Rico, Mayaguez, PR 00681, Puerto Rico.

Received Date: December 02, 2025 | Accepted Date: December 12, 2025 | Published Date: December 23, 2025

Citation: Lakshmi. N. Sridhar, (2025), Analysis and Control of a Transmission Model for Respiratory Syncytial Virus, *International Journal of Clinical Research and Reports*. 4(6); **DOI:** 10.31579/2835-785X/117

Copyright: © 2025, Dr. Lakshmi. N. Sridhar. This is an open-access article distributed under the terms of the Creative Commons Attribution License, which permits unrestricted use, distribution, and reproduction in any medium, provided the original author and source are credited.

Abstract

In this study, bifurcation analysis and multi-objective nonlinear model predictive control are performed on a transmission model for respiratory syncytial virus. Bifurcation analysis is a powerful mathematical tool used to deal with the nonlinear dynamics of any process. Several factors must be considered, and multiple objectives must be met simultaneously. The MATLAB program MATCONT was used to perform the bifurcation analysis. The MNLMPC calculations were performed using the optimization language PYOMO in conjunction with the state-of-the-art global optimization solvers IPOPT and BARON. The bifurcation analysis revealed the existence of branch points. The MNLMC converged to the utopia solution. The branch points (which cause multiple steady-state solutions from a singular point) are very beneficial because they enable the multi-objective nonlinear model predictive control calculations to converge to the Utopia point (the best possible solution) in the model.

Keywords: bifurcation; optimization; control; respiratory

Background

Respiratory Syncytial Virus (RSV) is one of the most significant causes of acute lower respiratory infections, especially in infants, young children, the elderly, and immunocompromised individuals. Its transmission dynamics, high infectivity, and ability to cause recurrent infections make it a major public health concern worldwide. Understanding the mechanisms and conditions that facilitate RSV transmission is crucial for developing preventive strategies, vaccines, and effective treatment plans. The transmission of RSV involves a complex interplay between viral biology, environmental factors, host immunity, and social behaviors that together determine the spread and impact of the infection within communities.

RSV is an enveloped, single-stranded, negative-sense RNA virus belonging to the *Paramyxoviridae* family and *Pneumo virus* genus. Its structural proteins, particularly the fusion (F) and attachment (G) glycoproteins, play critical roles in mediating viral entry into host cells and facilitating transmission. The F protein allows the virus to

fuse with the host cell membrane, while the G protein mediates attachment to respiratory epithelial cells. These surface proteins also enable RSV to spread directly between adjacent cells through a process known as syncytium formation, in which infected cells fuse with neighboring uninfected ones, creating large multinucleated cells that enhance viral dissemination without exposure to the extracellular environment. This mechanism allows the virus to evade some components of the immune response and increases its efficiency of transmission within the respiratory tract.

The primary route of RSV transmission is through direct or close contact with infectious respiratory secretions. When an infected individual coughs, sneezes, or talks, virus-containing droplets are expelled into the air. These droplets are generally large, typically greater than five micrometers in diameter, and therefore do not remain airborne for long distances. As a result, RSV transmission occurs mainly through short-range exposure, usually within one to two meters of an infected person. The virus can enter a new host

through the mucous membranes of the eyes, nose, or mouth when these droplets come into contact with them. In addition, RSV can survive for several hours on environmental surfaces such as toys, doorknobs, tables, or clothing, and for shorter periods on skin. Therefore, indirect contact, such as touching contaminated surfaces and then touching one's face, can also lead to infection. This combination of direct and indirect contact transmission makes RSV highly contagious, particularly in crowded or enclosed environments.

RSV infection often occurs in seasonal patterns, typically peaking during the winter months in temperate regions and during the rainy season in tropical climates. Environmental conditions such as lower humidity, cooler temperatures, and indoor crowding during these seasons contribute to increased transmission. The virus can remain viable longer in cool and dry conditions, while social behaviors such as spending more time indoors enhance person-to-person contact. In hospitals, nurseries, and daycare centers, outbreaks are particularly common, as young children and healthcare workers serve as reservoirs and vectors for viral spread. Nosocomial, or hospital-acquired, RSV infections can be severe and are a major concern in neonatal and pediatric intensive care units. Strict hygiene measures, including handwashing, surface disinfection, and the use of personal protective equipment, are critical in such settings to prevent outbreaks.

The incubation period of RSV—the time between exposure and the appearance of symptoms—is usually between two and eight days, with an average of about four to six days. During this time, the virus replicates in the epithelial cells of the upper respiratory tract, including the nasopharynx and trachea. Once symptomatic, infected individuals shed large quantities of the virus in nasal secretions, making them highly infectious. Viral shedding typically lasts for three to eight days in healthy adults, but can persist for several weeks in infants, the elderly, and immunocompromised individuals. This prolonged shedding in vulnerable populations significantly enhances the opportunity for community transmission and recurrent infections.

RSV transmission is particularly efficient in households with young children, who often serve as the initial point of infection. Infants and toddlers, especially those attending daycare, are exposed to multiple viral contacts and are more likely to transmit RSV to siblings, parents, and grandparents. In these settings, asymptomatic or mildly symptomatic carriers can still spread the virus effectively. Adults, who may experience only mild cold-like symptoms, often act as silent reservoirs of infection. Because immunity following RSV infection is incomplete and short-lived, reinfections occur throughout life, enabling the virus to circulate persistently in human populations.

Host factors also play a significant role in RSV transmission and disease severity. Infants younger than six months are at the highest risk for severe infection due to their underdeveloped immune systems and smaller airways. Premature infants, or those with underlying conditions such as congenital heart disease, chronic lung disease, or immune deficiencies, are particularly susceptible. The immaturity of the infant immune system limits the production of neutralizing

antibodies and effective T-cell responses, allowing more extensive viral replication and higher viral loads, which in turn increase transmissibility. The role of maternal antibodies is also important, as they provide partial protection in the first months of life, but this protection wanes rapidly, leaving infants vulnerable during the peak season for RSV transmission.

From a public health perspective, RSV transmission is challenging to control because it combines high infectivity with a lack of durable immunity. There is currently no fully licensed vaccine for RSV, though several candidates are in late-stage development, including maternal vaccines and monoclonal antibody-based prophylaxis for infants. Until these measures become widely available, non-pharmaceutical interventions remain the mainstay of prevention. These include frequent hand hygiene, avoiding close contact with sick individuals, cleaning surfaces and toys, and limiting exposure of infants to crowded places during RSV season. In healthcare settings, infection control protocols such as isolating infected patients, wearing gloves and masks, and enforcing strict hygiene procedures can significantly reduce transmission rates.

The introduction of monoclonal antibody prophylaxis, such as palivizumab, has provided partial protection for high-risk infants, reducing hospitalization rates but not completely preventing infection or transmission. Newer long-acting antibodies, like nirsevimab, have shown promise in extending protection for a full RSV season, potentially changing the epidemiology of transmission in infants once widely implemented. Similarly, maternal immunization strategies—where pregnant women are vaccinated to pass antibodies to their newborns—offer a promising approach to reduce early-life infection and viral spread in households.

In addition to individual preventive measures, understanding population-level transmission dynamics is essential. Mathematical modeling of RSV transmission indicates that community outbreaks are driven by a combination of seasonal factors, contact rates among children, and waning immunity. Public health surveillance helps identify the onset and intensity of RSV seasons, enabling hospitals and healthcare systems to prepare for increased admissions and implement preventive actions. School and daycare closures, though effective in reducing transmission during pandemics, are less feasible for RSV due to its annual recurrence and mild disease course in older children.

The transmission of Respiratory Syncytial Virus reflects the complex interactions between viral biology, human behavior, environmental factors, and host immunity. RSV spreads primarily through close contact with respiratory secretions and contaminated surfaces, thriving in settings where people, especially children, interact closely. Seasonal trends and the presence of prolonged viral shedding in vulnerable populations make control efforts difficult. Despite the absence of a universal vaccine, progress in monoclonal antibody therapies and maternal immunization holds promise for reducing both infection and transmission in the near future. Until such measures become broadly accessible, strict hygiene practices, public

awareness, and early detection remain the most effective tools in limiting RSV spread. Understanding the mechanisms of RSV transmission not only informs prevention strategies but also underscores the importance of continued research into vaccines and antiviral therapies to combat one of the most persistent respiratory pathogens affecting humanity.

Falsey et al (2000) [1] studied the respiratory syncytial virus infection in adults. Hall (2001) [2] investigated the connection between the respiratory syncytial virus and parainfluenza virus. White et al (2007) [3] provided an understanding of the transmission dynamics of respiratory syncytial virus using multiple time series and nested models. Sungchait et al (2022) [4], performed mathematical modeling and global stability analysis of super-spreading transmission of respiratory syncytial virus (RSV) disease. Kaler et al (2023) [5] provided a comprehensive review of the transmission, pathophysiology, and manifestation of the respiratory syncytial virus. Rosa et al (2023) [6] performed numerical fractional optimal control calculations of the respiratory syncytial virus infection. Abdullahi and Sule (2023) [7] developed a non-integer mathematical model of the respiratory syncytial virus. Jamil et al (2024) [8] performed qualitative analysis and chaotic behavior of respiratory syncytial virus infection in humans with a fractional operator. Awadalla et al (2024) [9] performed a fractional optimal control model and bifurcation calculations of human syncytial respiratory virus transmission dynamics. Al Ajlan et al (2025[10] performed mathematical Analysis and optimal control calculations of a transmission model for respiratory syncytial virus.

$$\begin{aligned}
 fac1 &= \beta1(z1)sv(1-u1) \\
 fac2 &= \beta2(z2)sv(1-u1) \\
 d(sv) &= \lambda - fac1 - fac2 - sv(\mu + u3) \\
 d(ev) &= fac1 + fac2 - ev\left(\frac{1}{\eta} + \mu + u3\right) \\
 d(z1) &= \frac{\rho}{\eta} ev - z1(\omega + \gamma1 + \mu + u2) \\
 d(z2) &= ev\frac{(1-\rho)}{\eta} + \omega(z1) - z2(\gamma2 + \mu + u2) \\
 d(rv) &= \gamma1(z1) + \gamma2(z2) - \mu(rv) + u3(sv + ev) + u2(z1 + z2)
 \end{aligned} \tag{1}$$

Bifurcation analysis

The MATLAB software MATCONT is used to perform the bifurcation calculations. Bifurcation analysis deals with multiple steady-states and limit cycles. Multiple steady states occur because of the existence of branch and limit points. Hopf bifurcation points

In this work, bifurcation analysis and multiobjective nonlinear model predictive control is performed on a transmission model for respiratory syncytial virus (Al Ajlan et al (2025[10]). The paper is organized as follows. First, the model equations are presented, followed by a discussion of the numerical techniques involving bifurcation analysis and multiobjective nonlinear model predictive control (MNLMP). The results and discussion are then presented, followed by the conclusions.

Model Equations (Al Ajlan et al, 2025 [10])

The variables sv , ev , $z1$, $z2$, rv represent susceptible, exposed, acutely infected, chronically infected, and recovered populations. The control and bifurcation parameters $u1$, $u2$, and $u3$ represent the isolation of infected individuals, the treatment of infected individuals, and the vaccination of susceptible individuals. The parameters $\lambda, \beta1, \beta2, \mu, \omega, \eta, \rho, \gamma1, \gamma2$ take on values 0.1, 0.1, 0.1, 0.03622, 0.1, 6, 0.3, 0.01, 0.1, and stand for the constant birth rate within the human population, the transmission rate of strain one, the transmission rate of strain two, the death rate of the human population, the rate of mutation of the virus from strain one to strain two, the incubation time of respiratory syncytial virus, the probability that strain one will infect a new case, the rate at which individuals infected with strain one recover, the rate at which individuals infected with strain two recover.

The model equations are

cause limit cycles. A commonly used MATLAB program that locates limit points, branch points, and Hopf bifurcation points is MATCONT (Dhooge, Govaerts, and Kuznetsov, 2003[11]; Dhooge, Govaerts, Kuznetsov, Mestrom and Riet, 2004[12]). This program detects Limit points (LP), branch points (BP), and Hopf bifurcation points(H) for an ODE system.

$$\frac{dx}{dt} = f(x, \alpha) \quad (2)$$

$x \in R^n$ Let the bifurcation parameter be α . Since the gradient is orthogonal to the tangent vector,

The tangent plane at any point $w = [w_1, w_2, w_3, w_4, \dots, w_{n+1}]$ must satisfy

$$Aw = 0 \quad (3)$$

Where A is

$$A = [\partial f / \partial x \quad | \quad \partial f / \partial \alpha] \quad (4)$$

where $\partial f / \partial x$ is the Jacobian matrix? For both limit and branch points, the Jacobian matrix $J = [\partial f / \partial x]$ must be singular.

For a limit point, there is only one tangent at the point of singularity. At this singular point, there is a single non-zero vector, y , where $Jy=0$. This vector is of dimension n . Since there is only one tangent the vector.

$$y = (y_1, y_2, y_3, y_4, \dots, y_n) \text{ must align with } \hat{w} = (w_1, w_2, w_3, w_4, \dots, w_n). \text{ Since} \\ J\hat{w} = Aw = 0 \quad (5)$$

the $n+1^{\text{th}}$ component of the tangent vector $w_{n+1} = 0$ at a limit point (LP).

For a branch point, there must exist two tangents at the singularity. Let the two tangents be z and w . This implies that

$$Az = 0 \\ Aw = 0 \quad (6)$$

Consider a vector v that is orthogonal to one of the tangents (say w). v can be expressed as a linear combination of z and w ($v = \alpha z + \beta w$). Since $Az = Aw = 0$; $Av = 0$ and since w and v are orthogonal,

$$w^T v = 0. \text{ Hence } Bv = \begin{bmatrix} A \\ w^T \end{bmatrix} v = 0 \text{ which implies that } B \text{ is singular.}$$

Hence, for a branch point (BP) the matrix $B = \begin{bmatrix} A \\ w^T \end{bmatrix}$ must be singular.

At a Hopf bifurcation point,

$$\det(2f_x(x, \alpha) @ I_n) = 0 \quad (7)$$

@ indicates the bialternate product while I_n is the n -square identity matrix. Hopf bifurcations cause limit cycles and should be eliminated because limit cycles make optimization and control tasks very difficult. More details can be found in Kuznetsov (1998[13]; 2009[14]) and Govaerts [2000] [15].

Multi-objective Nonlinear Model Predictive Control (MNL MPC)

The rigorous multi-objective nonlinear model predictive control (MNL MPC) method developed by Flores Tlacuahuaz et al (2012) [16] was used.

Consider a problem where the variables $\sum_{t_i=0}^{t_i=t_f} q_j(t_i)$ ($j=1, 2..n$) have to be optimized simultaneously for a dynamic problem

$$\frac{dx}{dt} = F(x, u) \quad (8)$$

t_f being the final time value, and n the total number of objective variables and u the control parameter. The single objective optimal control problem is solved individually optimizing each of the variables

$\sum_{t_i=0}^{t_i=t_f} q_j(t_i)$. The optimization of $\sum_{t_i=0}^{t_i=t_f} q_j(t_i)$ will lead to the values q_j^* . Then, the multiobjective optimal control (MOOC) problem that will be solved is

$$\begin{aligned} \min & \left(\sum_{j=1}^n \left(\sum_{t_i=0}^{t_i=t_f} q_j(t_i) - q_j^* \right) \right)^2 \\ \text{subject to} & \quad \frac{dx}{dt} = F(x, u); \end{aligned} \quad (9)$$

This will provide the values of u at various times. The first obtained control value of u is implemented and the rest are discarded. This procedure is repeated until the implemented and the first obtained control

values are the same or if the Utopia point where $\left(\sum_{t_i=0}^{t_i=t_f} q_j(t_i) = q_j^* \text{ for all } j \right)$ is obtained.

Pyomo (Hart et al, 2017) [17] is used for these calculations. Here, the differential equations are converted to a Nonlinear Program (NLP) using the orthogonal collocation method. The NLP is solved using IPOPT (Wächter And Biegler, 2006) [18] and confirmed as a global solution with BARON (Tawarmalani, M. and N. V. Sahinidis 2005) [19].

The steps of the algorithm are as follows,

1. Optimize $\sum_{t_i=0}^{t_i=t_f} q_j(t_i)$ and obtain q_j^* .
2. Minimize $\left(\sum_{j=1}^n \left(\sum_{t_i=0}^{t_i=t_f} q_j(t_i) - q_j^* \right) \right)^2$ and get the control values at various times.
3. Implement the first obtained control values
4. Repeat steps 1 to 3 until there is an insignificant difference between the implemented and the first obtained value of the control variables or if the Utopia point is achieved. The Utopia point is when

$$\sum_{t_i=0}^{t_i=t_f} q_j(t_i) = q_j^* \text{ for all } j.$$

Sridhar (2024) [20] demonstrated that when the bifurcation analysis revealed the presence of limit and branch points the MNLMPC calculations to converge to the Utopia solution. For this, the singularity condition, caused by the presence of the limit or branch points was imposed on the co-state equation (Upreti, 2013) [21].

If the minimization of q_1 lead to the value q_1^* and the minimization of q_2 lead to the value q_2^* . The MNLPMC calculations will minimize the function $(q_1 - q_1^*)^2 + (q_2 - q_2^*)^2$. The multiobjective optimal control problem is

$$\min (q_1 - q_1^*)^2 + (q_2 - q_2^*)^2 \quad \text{subject to} \quad \frac{dx}{dt} = F(x, u) \tag{10}$$

Differentiating the objective function results in

$$\frac{d}{dx_i} ((q_1 - q_1^*)^2 + (q_2 - q_2^*)^2) = 2(q_1 - q_1^*) \frac{d}{dx_i} (q_1 - q_1^*) + 2(q_2 - q_2^*) \frac{d}{dx_i} (q_2 - q_2^*) \tag{11}$$

The Utopia point requires that both $(q_1 - q_1^*)$ and $(q_2 - q_2^*)$ are zero. Hence

$$\frac{d}{dx_i} ((q_1 - q_1^*)^2 + (q_2 - q_2^*)^2) = 0 \tag{12}$$

The optimal control co-state equation (Upreti; 2013) [43] is

$$\frac{d}{dt} (\lambda_i) = -\frac{d}{dx_i} ((q_1 - q_1^*)^2 + (q_2 - q_2^*)^2) - f_x \lambda_i; \quad \lambda_i(t_f) = 0 \tag{13}$$

λ_i is the Lagrangian multiplier. t_f is the final time. The first term in this equation is 0 and hence

$$\frac{d}{dt} (\lambda_i) = -f_x \lambda_i; \quad \lambda_i(t_f) = 0 \tag{14}$$

At a limit or a branch point, for the set of ODE $\frac{dx}{dt} = f(x, u)$ f_x is singular. Hence there are two different vectors-values for $[\lambda_i]$ where $\frac{d}{dt} (\lambda_i) > 0$ and $\frac{d}{dt} (\lambda_i) < 0$. In between there is a vector $[\lambda_i]$ where $\frac{d}{dt} (\lambda_i) = 0$. This coupled with the boundary condition $\lambda_i(t_f) = 0$ will lead to $[\lambda_i] = 0$

Results and Discussion

u1, u2 and u3 were used as bifurcation parameters and each one of them produced branch points. When u1 was the bifurcation parameter, a branch point was found at (sv, ev, z1, z2, rv, u1) values of (2.760906, 0, 0, 0, 0, 0.493006) (Fig. 1a). When u2 was the

bifurcation parameter, a branch point was found at (sv, ev, z1, z2, rv, u2) values of (2.760906, 0, 0, 0, 0, 0.114105) (Fig. 1b). When u3 was the bifurcation parameter, a branch point was found at (sv, ev, z1, z2, rv, u3) values of (1.585122, 0, 0, 0, 1.175784, 0.026867) (Fig. 1c). These results indicate that the introduction of control parameters cause branch point bifurcations to appear.

For the MNLMPC, u1, u3 are the control parameters, and $\sum_{t=0}^{t_f} z1(t_i)$, $\sum_{t=0}^{t_f} z2(t_i)$ were minimized individually, and each led to a value of 0. The overall optimal control problem will involve the minimization of $(\sum_{t=0}^{t_f} z1(t_i) - 0)^2 + (\sum_{t=0}^{t_f} z2(t_i) - 0)^2$ was minimized subject to the equations governing the model. This led to a value of zero (the Utopia point).

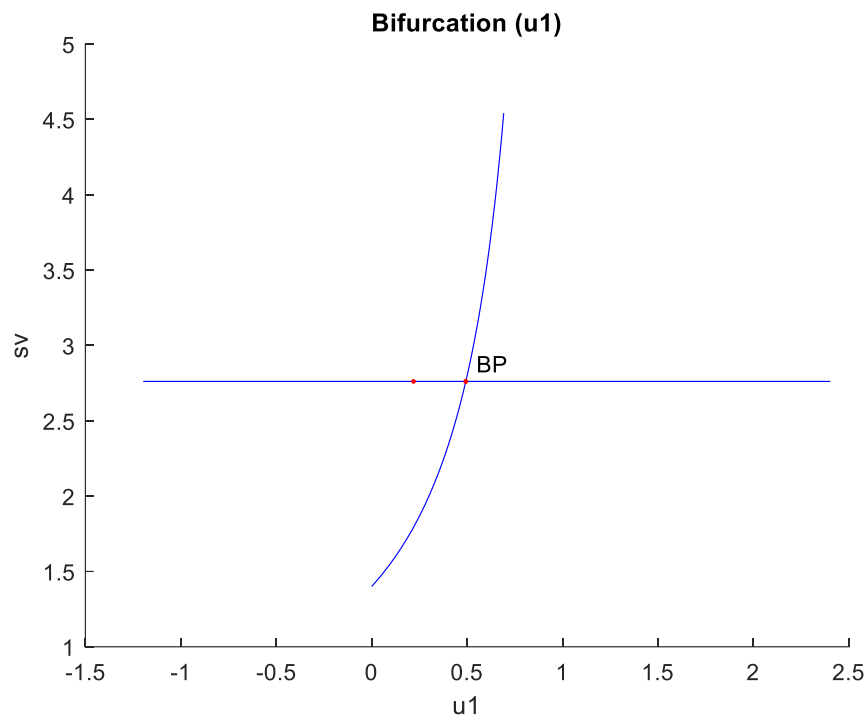


Figure 1a: u1 is the bifurcation parameter.

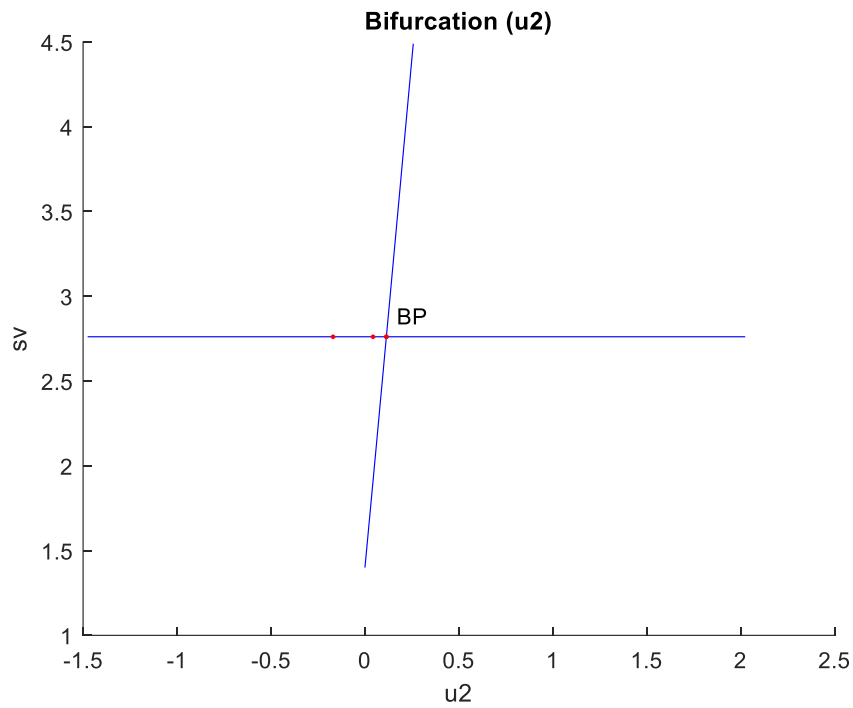


Figure 1b: u2 is the bifurcation parameter

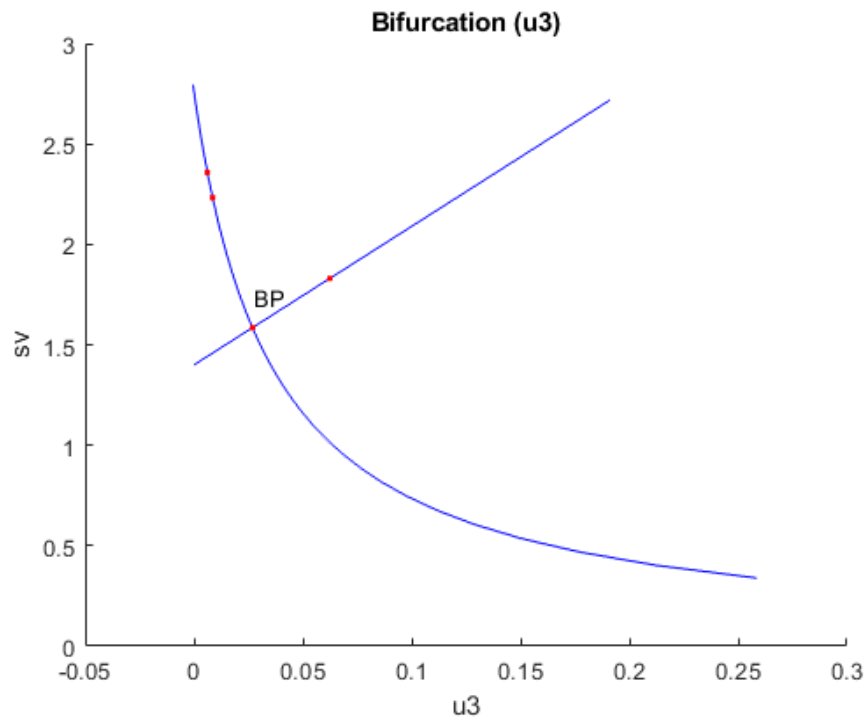


Figure 1c: u3 is the bifurcation parameter.

The MNLMPCC values of the control variables, u_1 , u_2 , and u_3 were 0.4992, 0.32099, and 0.06119. The MNLMPCC profiles are shown in Figs 2a-2d. The control profiles of u_1 , u_2 , and u_3 exhibited noise (Fig. 2c) and this was remedied using the Savitzky-Golay filter to produce the smooth profiles u_{1sg} , u_{2sg} , and u_{3sg} (Fig. 2d). The presence of the branch points causes the MNLMPCC calculations to attain the Utopia solution, validating the analysis of Sridhar (2024) [20].

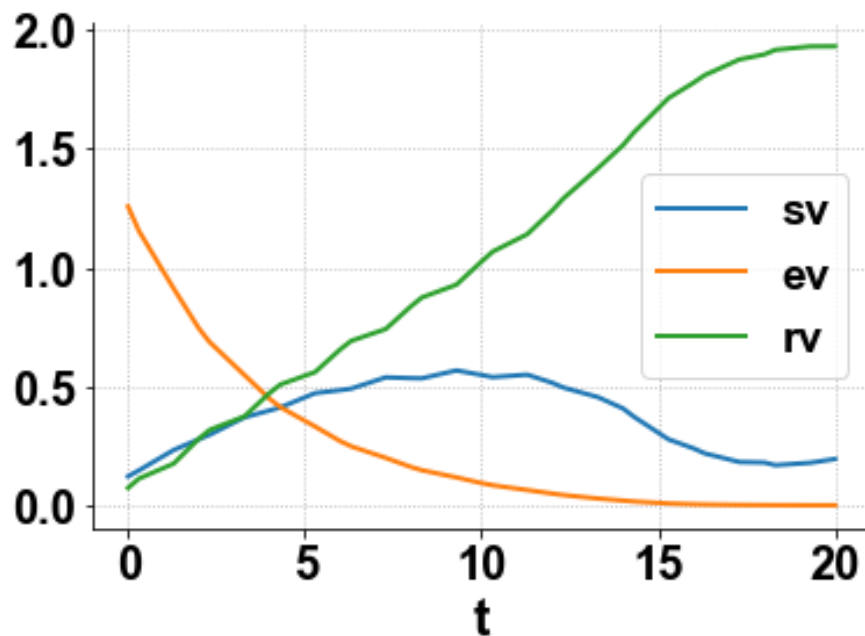


Figure 2a: MNLMPCC sv ev rv profiles.

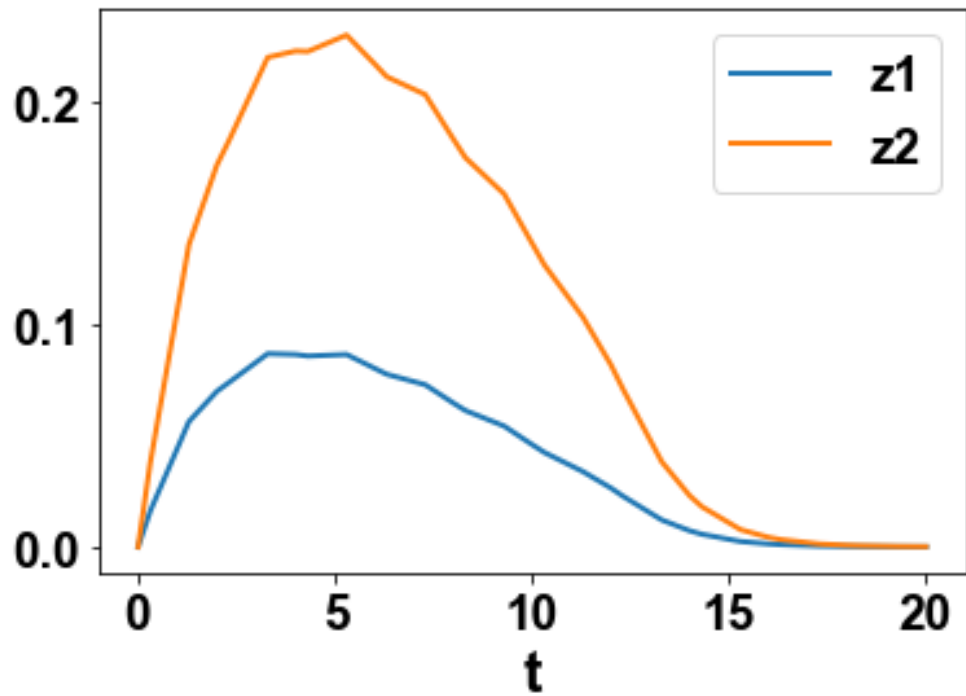


Figure 2b: MNLMPc z1 z2 profiles.

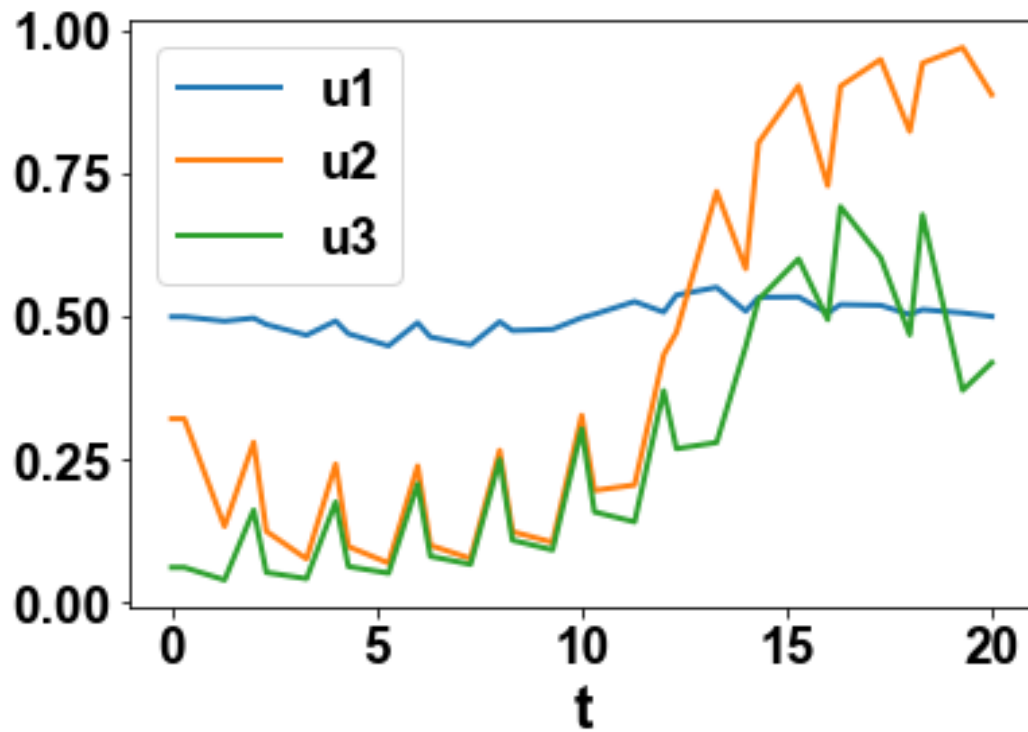


Figure 2c: MNLMPc u1 u2 u3 profiles.

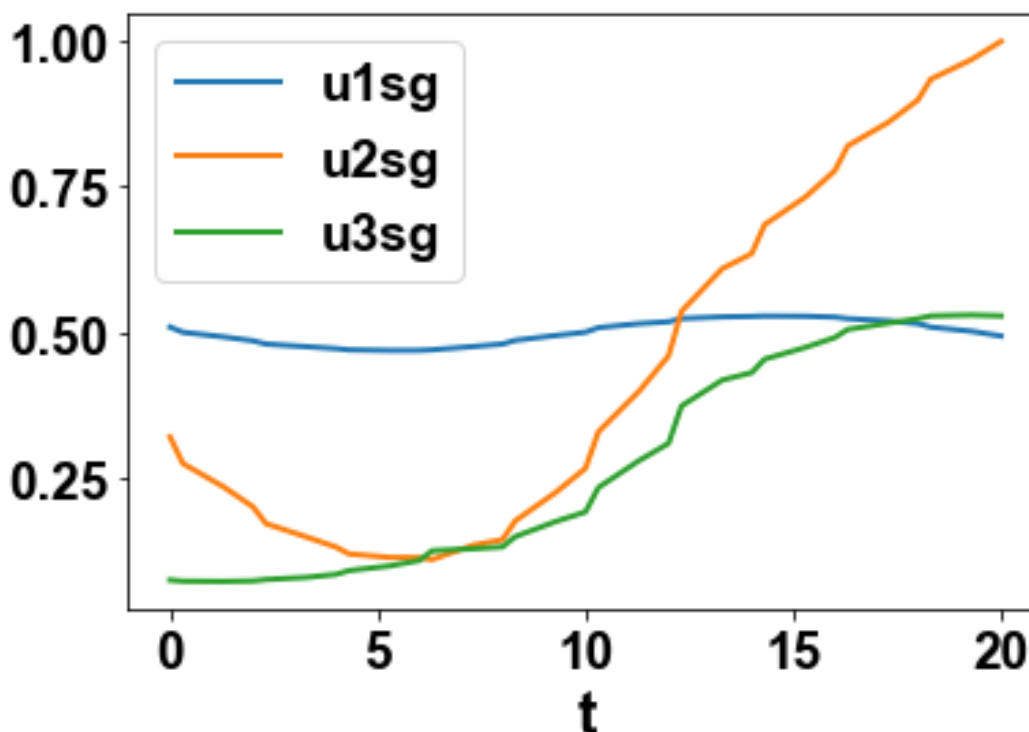


Figure 2d: MNLMPC u1sg u2sg u3sg profiles.

Conclusion

Bifurcation analysis and multi-objective nonlinear control (MNLMPC) studies on a transmission model for respiratory syncytial virus. The bifurcation analysis revealed the existence of branch points. These branch points (which cause multiple steady-state solutions from a singular point) are very beneficial because they enable the multi-objective nonlinear model predictive control calculations to converge to the Utopia point (the best possible solution) in the models. A combination of bifurcation analysis and Multi-objective Nonlinear Model Predictive Control (MNLMPC) on a transmission model for respiratory syncytial virus is the main contribution of this paper.

Data Availability Statement

All data used is presented in the paper

Conflict of interest

The author, Dr. Lakshmi N Sridhar has no conflict of interest.

Acknowledgement

Dr. Sridhar thanks Dr. Carlos Ramirez and Dr. Suleiman for encouraging him to write single-author papers

References

- Falsey, A.R.; Walsh, E.E. Respiratory syncytial virus infection in adults. *Clin. Microbiol. Rev.* 2000, 13, 371–384.
- Hall, C.B. Respiratory syncytial virus and parainfluenza virus. *N. Engl. J. Med.* 2001, 344, 1917–1928. Al Ajlan, Z.S
- White, L.J.; Mandl, J.N.; Gomes, M.G.M.; Bodley-Tickell, A.T.; Cane, P.A.; Perez-Brena, P.; Aguilar, J.C.; Siqueira, M.M.; Portes, S.A.; Straliotto, S.M.; et al. Understanding the transmission dynamics of respiratory syncytial virus using multiple time series and nested models. *Math. Biosci.* 2007, 209, 222–239.
- Sungchait, R.; Tang, I.-M.; Pongsumpun, P. Mathematical modeling: Global stability analysis of super spreading transmission of respiratory syncytial virus (RSV) disease. *Computation* 2022, 10, 120.
- Kaler, J.; Hussain, A.; Patel, K.; Hernandez, T.; Ray, S. Respiratory syncytial virus: A comprehensive review of transmission, pathophysiology, and manifestation. *Cureus* 2023, 15, e36342.
- Rosa, S.; Torres, D.F.M. Numerical fractional optimal control of respiratory syncytial virus infection in Octave/MATLAB. *Mathematics* 2023, 11, 1511.
- Abdullahi, M.B.; Sule, A. Non-integer mathematical model of respiratory syncytial virus. *Fudma J. Sci.* 2023, 7, 297–304.
- Jamil, S.; Bariq, A.; Farman, M.; Nisar, K.S.; Akgul, A.; Saleem, M.U. Qualitative analysis and chaotic behavior of respiratory syncytial virus infection in human with fractional operator. *Sci. Rep.* 2024, 14, 2175.
- Awadalla, M.; Alahmadi, J.; Cheneke, K.R.; Qureshi, S. Fractional optimal control model and bifurcation analysis of human syncytial respiratory virus transmission dynamics. *Fractal Fract.* 2024, 8, 44.

10. Al Ajlan, Z.S.; El-Shahed, M.; Alnafisah, Y. Mathematical Analysis and Optimal Control of a Transmission Model for Respiratory Syncytial Virus. *Mathematics* **2025**, *13*, 2929.
11. Dhooge, A., Govaerts, W., and Kuznetsov, A. Y., MATCONT: A Matlab package for numerical bifurcation analysis of ODEs, *ACM transactions on Mathematical software* 29(2) pp. 141-164, 2003.
12. Dhooge, A. W. Govaerts; Y. A. Kuznetsov, W. Mestrom, and A. M. Riet, CL_MATCONT; *A continuation toolbox in Matlab*, 2004.
13. Kuznetsov, Y. A. Elements of applied bifurcation theory. *Springer*, NY, 1998.
14. Kuznetsov, Y.A., (2009). Five lectures on numerical bifurcation analysis, *Utrecht University, NL*, 2009.
15. Govaerts, W. J. F., Numerical Methods for Bifurcations of Dynamical Equilibria, *SIAM*, 2000.
16. Flores-Tlacuahuac, A. Pilar Morales and Martin Riveral Toledo; Multiobjective Nonlinear model predictive control of a class of chemical reactors. *I & EC research*; 5891-5899, 2012.
17. Hart, William E., Carl D. Laird, Jean-Paul Watson, David L. Woodruff, Gabriel A. Hackebeil, Bethany L. Nicholson, and John D. Sirola. *Pyomo – Optimization Modeling in Python* Second Edition. Vol. 67.
18. Wächter, A., Biegler, L. “On the implementation of an interior-point filter line-search algorithm for large-scale nonlinear programming. *Math. Program.* 106, 25–57 (2006).
19. Tawarmalani, M. and N. V. Sahinidis, A polyhedral branch-and-cut approach to global optimization, *Mathematical Programming*, 103(2), 225-249, 2005
20. Sridhar LN. (2024), Coupling Bifurcation Analysis and Multiobjective Nonlinear Model Predictive Control. *Austin Chem Eng.* 2024; 10(3): 1107.
21. Upreti, Simant Ranjan (2013); *Optimal control for chemical engineers*. Taylor and Francis.

Ready to submit your research? Choose ClinicSearch and benefit from:

- fast, convenient online submission
- rigorous peer review by experienced research in your field
- rapid publication on acceptance
- authors retain copyrights
- unique DOI for all articles
- immediate, unrestricted online access

At ClinicSearch, research is always in progress.

Learn more <https://clinicsearchonline.org/journals/international-journal-of-clinical-research-and-reports>



© The Author(s) 2023. **Open Access** This article is licensed under a Creative Commons Attribution 4.0 International License, which permits use, sharing, adaptation, distribution and reproduction in any medium or format, as long as you give appropriate credit to the original author(s) and the source, provide a link to the Creative Commons licence, and indicate if changes were made. The images or other third party material in this article are included in the article's Creative Commons licence, unless indicated otherwise in a credit line to the material. If material is not included in the article's Creative Commons licence and your intended use is not permitted by statutory regulation or exceeds the permitted use, you will need to obtain permission directly from the copyright holder. To view a copy of this licence, visit <http://creativecommons.org/licenses/by/4.0/>. The Creative Commons Public Domain Dedication waiver (<http://creativecommons.org/publicdomain/zero/1.0/>) applies to the data made available in this article, unless otherwise stated in a credit line to the data.